



Entropy, Exergy and Entransy Analyses on Fabricated Shell and Spiral Tube Heat Exchanger

Ankur Geete¹ · Ankur Bhattacharjee¹ · Abhishek Patwa¹ · Krishnam Pandey¹

Received: 20 August 2019 / Accepted: 2 April 2021 / Published online: 23 April 2021
© The Institution of Engineers (India) 2021

Abstract In this exploratory attempt, shell-spiral tube heat exchanger is constructed. Entropy, exergy and entransy concepts are applied to examine the performance of constructed heat exchanger at different flow rates and inlet temperatures of hot and cold fluids. Theoretically, Reynolds and Nusselt numbers are calculated with convective heat transfer coefficient and pressure drop through the spiral tube. Rates of entropy generation, exergy destruction, entransy dissipation, entransy dissipation based thermal resistances, entransy dissipation and entropy generation numbers are assessed for the constructed spiral tube heat exchanger through investigational outputs. Percentage augmentations and decrements are also found for the performance assessment properties to be acquainted with maximum or minimum augmentation/decrement at the equivalent flow rates of fluids. These experimental analyses are accomplished as: the highest effectiveness is 0.988 with the least entransy dissipation rate which is 224.171 W K. Entransy dissipation based thermal resistance is 0.013 K/W and the entransy dissipation number is 0.052 that are enhanced circumstances for a heat exchanger. After analyses, those working circumstances are recommended which provide smallest amount of entropy, exergy and entransy losses, but effectiveness ought to be as high as achievable. The advised conditions from these investigation efforts are; hot/cold fluid flow rates should be 0.001/0.037 kg/s and inlet temperatures should be 59/26.8 °C respectively, for this experimental work.

Keywords Entropy analysis · Exergy analysis · Entransy analysis · Shell-spiral tube heat exchanger

List of Symbols

C	Specific heat of the fluid in J/kg-K
D_i	Spiral tube inner diameter in m
dP	Spiral tube side pressure drop in flowing fluid in N/m ²
EG	Entropy generation in W/K
EGN	Entropy generation number
EnD	Entransy dissipation in W K
EnDTR	Entransy dissipation based thermal resistance in K/W
EnDn	Entransy dissipation number
f	Friction factor consider for spiral tube side
G	Entransy in W K
h	Convective heat transfer coefficient for spiral tube side fluid in W/m ² K
K	Thermal conductivity of the spiral tube side fluid in W/m-K
L	Spiral tube length in m
m	Mass flow rate of the fluid in kg/s
N_{egn}	Entropy generation number
NOF	Number of passes
Nu	Nusselt number for the spiral tube side fluid
Pr	Prandlt number for the spiral tube side fluid
Q	Heat transfer rate through fabricated shell-spiral tube heat exchanger in W
Q'	Stored electrical charge in W
Re	Reynolds number for the spiral tube side fluid
R	Thermal resistance in K/W
S	Entropy of the system in W/K
SSTHEX	Shell-spiral tube heat exchanger
T	Temperature in K

✉ Ankur Geete
ankur_geete@yahoo.co.in

¹ Mechanical Engineering Department, Sushila Devi Bansal College of Technology, Indore 453331, Madhya Pradesh, India

U	Stored heat or internal energy of the system in W
V'	Voltage in V
V	Fluid velocity inside the spiral tube in m/s

Greek Symbols

μ	Dynamic viscosity of the spiral tube side fluid in N s/m ²
ρ	Density of fluid in the spiral tube in kg/m ³
ψ	Rate of exergy destruction in W

Subscripts

h	Hot fluid
c	Cold fluid
i	Inlet condition
o	Outlet condition
ed	Entransy dissipation
egn	Entransy dissipation number
max	Maximum condition
edtr	Entransy dissipation based thermal resistance
gen	Generation
0	Ambient conditions

Introduction

The heat exchanger is an apparatus that transfers heat from one fluid to another. It was introduced near the commencement of 1900s to complete the requisite of heat/energy in the power plants and other industries through enormous heat exchanging surfaces like condensers and feed water heaters. These enormous heat exchanging devices are proficient to work under relatively high pressure ranges. For these purposes, shell-spiral tube heat exchangers are universally employed in the power generation, chemical, refrigeration and air-conditioning industries [1, 2]. But the design of shell-spiral tube heat exchanger is more sophisticated and more sensitive. Numerous varieties of heat exchangers have been designed [3–6] and developed which could be classified on the basis of—(1) nature of the heat exchanging process (i.e. Direct and indirect contacts—regenerators and recuperators), (2) relative direction of fluid flow (i.e. Parallel, counter and cross flow), (3) design and constructional features (i.e. Concentric tube, shell-tube, multiple shell-tube passes and compact heat exchangers—plate fin) and (4) physical state of fluids (i.e. Condensers and evaporators) [1, 2]. For this research work, shell-spiral tube type heat exchanger is elected which consists of the following essential components; (a) Tube—In this heat exchanger, heat is transferred through the outer surface of the tube therefore highly thermal conductive materials; copper, aluminum and brass as tube materials are recommended. In this experimental work, copper is utilized as spiral tube material that shown

in Fig. 1 [3, 4]. (b) Tube sheet—It is a circular metal disc which holds the tubes at the ends. It also has grooves for the gaskets and the holes for the flange bolts [3, 4]. (c) Shell—Tubes are placed within the shell. It contains shell side fluid and also has nozzles at inlet and outlet ports [4, 5], (d) Channel cover—It is a disc that is used to bolt the channel flange and it can be detached for the inspection of the tubes without any disturbance in the tube side arrangement [5, 6], and (e) Baffle—Baffles are used to guide the fluid which is flowing through the shell to augment the velocity, turbulence and then heat transfer coefficient. Baffles are also employed to hold the long tubes in the shell [5, 6]. Different components of the shell-spiral tube heat exchanger (SSTHEx) are publicized in Fig. 2. Numbers of researchers have done work on entropy model (i.e. entropy generation rate and entropy generation number) for a variety of thermal systems and their efforts have been discussed as; Chen et al. [7] worked on an irreversible light driven engine to minimize the rate of entropy generation through linear phenomenological heat transfer law. Chen et al. [8] diminished the rate entropy generation for isothermal crystallization process by generalized mass diffusion law. Chen et al. [9] also initiated the approaches to decrease the rate of entropy generation for the hydrogenation of CO₂ to light olefins. Bejan [10] did lot of work on entropy generation for heat and fluid flow. Geete [11] analysed the rates of exergy, entransy and entransy based thermal resistances for double pipe heat exchanger with dissimilar pipe materials. Paniagua et al. [12] estimated the rates of exergy destruction with a new simple method for various heat exchangers. Exergy model (i.e. exergy at inlet, exergy at outlet, exergy gain rate, exergy destruction rate and exergy efficiency) has been adopted for performance analyses and entransy model (i.e. entransy dissipation rate, entransy dissipation based thermal resistance and entransy dissipation number) has also been applied to various thermal systems at different operating/working environments. Analyses on exergy and entransy have been presented here; Chen et al. [13] optimized the heat and mass transfer

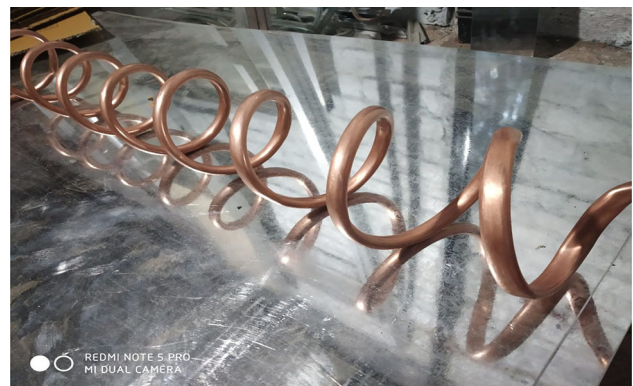


Fig. 1 Spiral tube (copper) for fabricated heat exchanger

Fig. 2 Different components manufactured for heat exchanger



processes on the basis of the entransy dissipation minimization concept. Cheng et al. [14] found the various losses of heat transfer and heat-work conversion processes and they have also done different analyses which were based on entransy theory. Feng et al. [15] minimized/optimized the rates of entransy dissipation for + shaped high conductivity channels. Guo et al. [16] described the term entransy which is a physical quantity and entransy shows heat transfer ability for any heat exchanging devices. Wang and Zhu [17] analysed the air preheater with multi stage LHS unit based on the entrance dissipation minimization concept. Guo et al. [18] evaluated the performance of the heat exchanger by entransy dissipation concept and for that they applied entransy dissipation number. Kim and Kim [19] optimized the design of heat exchanger by adopting the entransy dissipation minimization theory. Some research works have also been done on the helical tube heat exchangers. Liu et al. [20] proposed novel helical coiled heat exchanger in the heat pump system and investigated thermal/hydrodynamic performance of the heat exchanger with different coil diameters and pitches. They found pumping power and pressure drop increase with the flow rate, and thermal performance of the heat exchanger increases with coil pitch but decreases with coil diameter. Bakir et al. [21] optimized and evaluated the NTU-effectiveness of helical coil tube heat exchanger with the air bubble injection method. They concluded the heat transfer resistance decreases and thermal performance of heat exchanger increases with the air bubble injection process. Abu-Hamdeh et al. [22] also analysed the performance of helical coil tube heat exchanger on the basis of the thermal and hydraulic parameters. They recommended semicircular cross section sector-by-sector heat exchanger which gives better performance than the quadrant circular cross section and tube in tube heat exchangers. Kumar and Chandrasekar [23] reviewed some research work on helical coil heat exchanger where several specific nanofluids were used as flowing fluids. Wang et al. [24] compared the experimental

and numerical results of the various helical coil tube heat exchangers. After investigations, they concluded the helically coiled-twisted trilobal tube heat exchanger performs better on the hydraulic and thermal basis than helically coiled elliptical tube, helically coiled plain tube and trilobal tube heat exchangers. Kumar and Chandrasekar [25] investigated heat and flow characteristics of double helically coiled tube heat exchanger using ANSYS 14.5 software where MWCNT/water nanofluids at 0.2%, 0.4% and 0.6% volume concentrations used as flowing fluid. They found 7.2% deviation of Nusselt number and 8.5% deviation of pressure drop between the CFD and experimental outputs. Mirgolbabaee [26] analysed the thermal performance of vertical helically coiled tube heat exchanger at different shell side flow rates, coil-to-tube diameter ratios and coil pitches. Correlation for effectiveness-NTU of vertical helically coiled tube heat exchanger was also established. Wang et al. [27] studied the heat transfer and flow characteristics of shell side fluid for helically coiled tube heat exchanger, experimentally and numerically. They proposed a novel algorithm called double layer multi objective optimization and also suggested new correlations for the heat transfer and flow resistance of the shell side. Solanki and Kumar [28] found the frictional pressure drop characteristics of R-600a fluid which was flowing inside the horizontal smooth and dimpled helical coiled tube shell type heat exchanger. They concluded frictional pressure drop increases with mass flux and vapour quality, pressure drop decreases when the saturation temperature increases and the performance factor decreases when the vapour quality and mass flux increase. Han et al. [29] applied entropy generation theory on helically coiled tube heat exchanger for multi-objective optimization. They developed correlations to calculate the entropy generation number for that heat exchanger under three different conditions. Gholamalizadeh et al. [30] compared the performance of helically coiled tube heat exchanger with different shapes of coiled copper wires which inserted in

the heat exchanger. They calculated the Nusselt number and friction factor increase to 340.9% and 536.1% by inserting circular cross section coiled copper wire in the heat exchanger. Saydam et al. [31] designed, fabricated and experimentally analysed the performance of the helical coil heat exchanger with the phase changing material at different inlet temperatures, flow directions and flow rates. They searched out by the experiments that the charging time reduces by 35% when the inlet temperature of hot fluid increases from 70 to 75 °C and similarly the charging time decreases by 21% when the flow rate increases from 0.5 to 4 L/min. Wang et al. [32] studied heat transfer and flow characteristics of the shell side fluid for the helically coiled trilobal tube heat exchanger. They found 1.16 to 1.36 times better heat transfer performance as compare to helically coiled plain tube heat exchanger and friction factor also increased about 0.96 to 1.1 times. Sheeba et al. [33] also investigated the thermal performance of a helical coil heat exchanger and proposed a correlation to calculate the Nusselt number in terms of Dean number, Prandtl number and pitch. Omidi et al. [34] analysed the effects of physical and geometric parameters on the performance of the helical coil heat exchanger using various lobed cross sections. They found the helical coil with six lobes shows better outputs in terms of the highest Nusselt number and the lowest friction factor as compare to other lobes. Mohapatra et al. [35] optimized the performance of three fluids heat exchanger with different design parameters. Maximum heat transfer rate and minimum pressure drop for the heat exchanger were achieved by the Taguchi based optimization technique. Kareem [36] optimized the double pipe helical tube heat exchanger and compared its outputs with straight double tube heat exchanger on ANSYS FLUENT 14 under turbulent flow conditions. They also found the best cross section of the helical coil and recommended tapered cross section of the coil which gives better performance. Kong et al. [37] found various heat transfer characteristics of deionized water based graphene nanofluid which was used as flowing fluid in the vertical helical coiled counter flow heat exchanger at various coil dimensions. They achieved better performance from the heat exchanger with high thermal conductivity and low specific heat capacity of the nanofluid. Verma et al. [38] improved heat transfer rate and frictional losses in the heat exchanger pipe through the modified helical coiled insert. They found experimentally the Nusselt number and friction factor enhance in the range of 1.49–3.14 and 11.2–19.9 with modified helical coil insert (as compare to smooth pipe). Moghadam et al. [39] analyzed thermo/hydraulic properties of the turbulent TiO_2/W -EG nanofluid which flows inside the double pipe heat exchanger and also optimized the performance with helical coil insert in the pipe through genetic algorithms. Elattar et al. [40]

investigated thermal and hydraulic performance analyses for multi tube in tube heat exchanger at different operating and geometrical parameters. They developed correlations for coil pumping power, effectiveness and thermal/hydraulic index. Ghorbani et al. [41] studied the thermal performance of shell and coil heat exchanger at different tube diameters, coil pitches, shell-side and tube-side mass flow rates experimentally. They found the same correlation for $\varepsilon - \text{NTU}$ for the mixed convection heat exchanger as a pure counter-flow heat exchanger. Fouda et al. [42] analysed the thermal performance of multi tube in tube helical coiled heat exchangers through modeling. After comparison they concluded the multi tube in tube helical coiled heat exchangers give better outputs than other heat exchangers. In this research effort shell-spiral tube heat exchanger is fabricated in the workshop. A computer generated model is shown in Fig. 3 and the fabricated SSTHEx is also revealed in Fig. 4. The dimensions of the fabricated heat exchanger are; shell diameter is 127 mm, shell length is 800 mm, baffle cut is 25%, baffle spacing is 100 mm, number of tube and number of passes are one, required heat transfer area is 1.16 m^2 , pitch ratio is 3.1 and number of baffles are 7. Reynolds number, Nusselt number, friction factor, convective heat transfer coefficient and pressure drop through the spiral tube are calculated hypothetically. Afterward rates of entropy generation (EG), rates of exergy destruction (ExD), rates of entransy dissipation (EnD), entransy dissipation based thermal resistances (EnDTRs), entransy dissipation numbers (EnDns) and entropy generation numbers (EGNs) are found experimentally with effectiveness for the fabricated SSTHEx at different flow rates and inlet temperatures of hot and cold fluids. Percentage changes in the effectiveness, rates of EG, ExD, EnD, EnDTR, EnD and EGN are also determined to distinguish the highest or smallest amount of increment/decrement in the performance assessment characteristics through a range of experimental analyses.

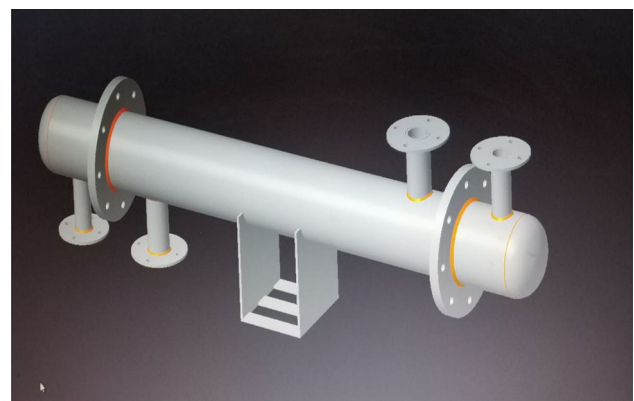


Fig. 3 Computer software generated model of heat exchanger



Fig. 4 Fabricated shell and spiral tube heat exchanger

Methodology

During this work, tube side analyses are done through several empirical relations and the relations are given below from Eqs. 1–6 [1–6]. The relation between the Reynolds number, density, velocity, inner diameter of the tube and dynamic viscosity has been presented by Eq. 1 [1, 2]. There are two mathematical equations for the Nusselt number that distinguished via the types of flow; if the flow is turbulent, the relation was given by Petukhov-Kirillov as Eq. 2 [2, 3], and if the flow is laminar then the relation was given by researchers Sieder and Tate as Eq. 4 [2, 3]. Here f is the friction factor which can be found by Eq. 3. Reynolds and Nusselt numbers can be calculated by Eqs. 1–4 [1–3].

$$Re = (\rho V D_i) / (\mu) \tag{1}$$

$$Nu = \left\{ \frac{(f/2)(Re Pr)}{1.07 + 12.7(f/2)^{0.5} \left(Pr - 1 \right)} \right\} \tag{2}$$

$$f = (1.58 \ln(Re) - 3.28)^{-2} \tag{3}$$

$$Nu = 1.86(Re Pr D_i/L)^{0.33} \tag{4}$$

In this research work, hypothetical estimation of the heat transfer coefficient for the spiral tube side is completed through the succeeding relation as in Eq. 5 [4–6].

$$h = (Nu K) / D_i \tag{5}$$

The pressure drop in the spiral tube side flowing fluid is calculated through the number of passes in the heat exchanger and the dimensions of the spiral tube. Consequently, the spiral tube side pressure drop is evaluated with Eq. 6 [3–6].

$$dP = \left\{ \frac{4fL(NOP)}{D_i} + 4(NOP) \right\} \left\{ \rho V^2 / 2 \right\} \tag{6}$$

Afterward the above hypothetical analysis, SSTHEx is fabricated and followed by numbers of experiments are carried out to assess the performance of fabricated heat

exchanger at different environments. Entropy, exergy and entransy analyses are accomplished for the performance finding of heat exchanger by experimental outputs [45–50]. These three imperative terms can be enlightened as; (i) Entropy—Entropy is the thermodynamic property which characterizes the unavailable energy of the thermodynamic system [48–50]. (ii) Exergy—Exergy/available energy is the maximum quantity of work that will be obtained during a reversible thermodynamic process whilst process starts from the definite surroundings (P, T) to ends at the atmospheric conditions (P_0, T_0) reversibly [51, 52]. And (iii) Entransy—Entransy term is proposed through the equivalence of heat conduction with electrical conduction. The entransy of a thermodynamic system is also enlightened by various investigators as it is the capacity of heat transfer through the heat exchanging system [18, 45, 47]. Information regarding heat engine/pump or refrigerator is obtained by the second law of thermodynamics for a cyclic process. Furthermore, if this is applied for a process, then entropy as a thermodynamic property is introduced [44]. It is observed by the researchers that the entropy is generated during an irreversible thermodynamic process since the quantity of change in entropy for that irreversible process will be more than the quantity which could be obtained by the integration of (dQ/T) [8–10, 44]. They have also concluded that the generation of entropy is due to internal irreversibility or dissipative work during a thermodynamic process [44]. The rate of EG is positive for real process (i.e. irreversible/actual process) and it is zero for a reversible/hypothetical process [7–12]. Irreversibility/losses are found for the fabricated SSTHEx as a thermodynamic system by the following Eq. 7 [44, 47].

$$TS_{gen} = m_h C_h f(T_h) + m_c C_c f(T_c) \tag{7}$$

If the thermodynamic system attains thermodynamic equilibrium state with its surrounding (i.e. T_0, P_0 ; dead state) in that case the maximum possible work can be obtained from the thermodynamic system. This maximum work is acknowledged as exergy or available energy of that system [44]. Investigators have concluded that the actual work transfer from the system is always less than the work that can be achieved through reversibly. The deviation between reversible and actual work transfer is accepted as losses from the system due to irreversibility [11, 44, 45]. Destruction in the exergy was introduced by Gouy-Stodola as $T_0 S_{gen}$ term [44, 45, 48, 49]. In a thermodynamic process, the rate of exergy losses/ExD is directly proportional to the EG rate and the temperature of the surrounding. The rates of ExD (ψ) for SSTHEx are found by the Eq. 8 [50–52].

Table 1 Explanation of entransy concept by equivalence between electrical and thermal parameters [11, 14, 16]

Electric potential (V)	Electric flux (Amp)	Electric resistance
V'	I	$R_{\text{elect. (or } V'/I)}$
Thermal potential (Kelvin)	Heat flux (W)	Thermal resistance
T	Q	$R_{\text{thermal (or } T/Q)}$
Electricity transfer rate (A)	Ohm's Law	Electrical Charge Stored
I	$I = K_e A (dV/dn)$	Q'
Heat Transfer Rate q (W)	Fourier's Law $Q = K A (dT/dn)$	Heat Stored U (or $m c_v T$)
Capacitance $C_e = Q'/V'$		Thermal Capacity $C = U/T$
Electrical potential energy stored in a capacitor $E_e = Q'V'/2$		Thermal potential energy stored in a body $E = UT/2$

$$\text{Rate of ExD; } \psi = [m_h C_h \{(T_{hi} - T_{ho}) - T_0 \ln(T_{hi}/T_{ho})\}] - [m_c C_c \{(T_{co} - T_{ci}) - T_0 \ln(T_{co}/T_{ci})\}] \quad (8)$$

The performance analyses of SSTHEX at various conditions are also done by the entransy which was established through the correlations between the electrical and thermal parameters as revealed in Table 1 [49–51].

From the Table 1 it has been seen that the electrical potential stored energy in the capacitor is $Q'V'/2$ and the thermal potential stored energy in the system is $UT/2$. Now, the entransy term (G) was specified by the researchers as the half of the product of the internal energy (U) and temperature (T) that can be written as Eq. 9 [16]. The entransy losses can also be calculated in terms of EnD rate, which is the association between the flow rates, specific heats and inlet/outlet temperatures of the flowing fluids as Eq. 10 [14, 49–51];

$$G = 1/2 UT \quad (9)$$

$$G_{\text{ed}} = 1/2 [m_h C_h \{(T_{hi})^2 - (T_{ho})^2\}] - 1/2 [m_c C_c \{(T_{co})^2 - (T_{ci})^2\}] \quad (10)$$

The EnDTR for SSTHEX is estimated by the calculated EnD rate and the heat transfer rate through the fabricated heat exchanger experimentally. This thermal resistance should be least for a heat exchanger and can be defined as the ratio of EnD rate to the square of the heat transfer rate as in Eq. 11 [51, 52].

$$R_{\text{edtr}} = G_{\text{ed}}/Q^2 \quad (11)$$

Investigators have completed additional exploration and introduced a novel dimensionless term which is called entransy dissipation number (i.e. EnDn) [18]. This dimensionless number is also implemented for the performance analysis of SSTHEX. EnDn can be described as the ratio of the EnD rate to the product of the rate of heat transfer and the highest achievable temperature difference between hot–cold fluids through a heat exchanger. This temperature difference can be reached for the heat exchanger with extreme temperatures of the hot and cold fluids (i.e. T_{hi} and T_{ci}). Entransy dissipation number can be found by Eq. 12 [18] and this equation can also be expressed in terms of effectiveness as Eqs. 14–15. Effectiveness is the ratio of the actual rate of heat transfer (Q) to the highest achievable rate of heat transfer (Q_{max}) [43] through SSTHEX as Eq. 13 with hot and cold fluids respectively [43, 44].

$$\text{EDN} = G_{\text{ed}}/[Q(T_{hi} - T_{ci})] \quad (12)$$

$$\varepsilon = (Q)/(Q_{\text{max}}) \quad (13)$$

$$\text{EDN} = G_{\text{ed}}/[\varepsilon Q_{\text{max}}(T_{hi} - T_{ci})] \quad (14)$$

$$\text{or EDN} = G_{\text{ed}}/[\varepsilon(m_f C_f)_{\text{min}}(T_{hi} - T_{ci})^2] \quad (15)$$

In this experimental work, EG rates (S_{gen}) and EGNs (N_{egn}) are also calculated for the fabricated SSTHEX. EGN can be defined as the ratio of the rate of EG to the lowest achievable EG rate or the lowest heat capacity of the fluid which is flowing through a fabricated heat exchanger [12] and it can be expressed as in Eq. 16.

$$N_{egn} = S_{gen}/(mC)_{min} \tag{16}$$

Results with Experimental Analyses

In this research work, fabrication of the heat exchanger is done in the workshop, the shell is made out of mild steel and spiral tube made from copper. Theoretical analyses are done for the shell and spiral tube heat exchanger in this work additionally. Length of the spiral tube, pitch of the tube, tube side Reynolds’s number, pressure drop, Nusselt number, Prandlt number and convective heat transfer coefficient are found and the outputs are shown in Table 2. In these analyses, following properties are considered as shown in Table 3. Fourteen various experiments are performed on SSTHEx at different flow rates and inlet temperatures of hot and cold fluids. Measured flow rates and outlet temperatures of both fluids with calculated effectiveness are shown in Table 4. EG rates, ExD rates, EnD rates, EnDTRs, EnDns and EGNs at different operating conditions are also shown in Table 5.

From experimental results, it is observed that maximum effectiveness (i.e. 0.988) from heat exchanger was achieved with the minimum EnD rate, EnDTR and EnDn but minimum effectiveness (i.e. 0.781) and the temperature decrement in hot fluid were found at 0.032 and 0.0066 kg/s flow rates. Highest temperature decrement in hot fluid (i.e. 36.4 °C) was observed with maximum EGN. Extreme temperature increment in cold fluid (i.e. 5.3 °C) was achieved with supreme rates of ExD and EnD. Lowest increment was found at least rate of EG and EGN with maximum EnDn. Least rates of ExD and EG can be found with the most EnDTR and EnDn. It is also observed from output that highest percentage increment (i.e. 5.67%) in the outlet temperature of hot fluid occurs at 0.028 and 0.0012 kg/s flow rates but lowest increment occurs at 0.037 and 0.001 kg/s flow rates. The effects of percentage increments in the hot fluid outlet temperature on effectiveness, EG rate, EnD rate and EGN are shown in Fig. 5.

The following results are also analysed; (1) maximum percentage changes in the temperature increment of cold

fluid (i.e. 7.547%) and effectiveness (i.e. 7.364%) but least change in the rate of EnD were found at same flow rates of fluids (i.e. 0.018/0.0006 kg/s). (2) Lowest percentage changes in the temperature decrement for hot fluid, effectiveness and the rate of ExD but extreme changes in the rate of EnD, the EnDTR and the EnDn were occurred at same flow rates (i.e. 0.037/0.001 kg/s) of fluids. (3) Maximum percentage changes in the rate of EG (i.e. 313.33%) and the EGN (i.e. 300.0%) both were evaluated at same flow rates (i.e. 0.0184/0.0018 kg/s) but minimum changes in the rate of EG and EGN were found at different flow rates. (4) Highest percentage changes in the rate of ExD (i.e. 26.095%) but minimum changes in the EnDTR (i.e. 17.647%) and in the EnDn (i.e. 21.982%) were found at 0.032/0.0066 kg/s flow rates.

Utmost grow in the temperature of cold fluid is found in experiment number 5 that shows maximum flow rates with greater rates of ExD and EnD which are not favorable situations for better outputs. Smallest rates of EG, ExD and EGN are achieved in experiment number 10 that shows minimum flow rates of hot/cold fluids which are better conditions but smallest increment in the temperature of cold fluid with the highest EnDn and thermal resistance were found in the same experiment and these conditions are adverse. So here two contradicting conditions are seen; one is the least ExD-EG rates which are excellent and the other is the utmost thermal resistance-EnDn which are undesirable for a heat exchanger. It is also observed that when the outlet temperature of hot fluid increases, then effectiveness and EnD rate decrease but the EG rate and EGN generally increase at the same flow rates the fluids. Highest increments in the EnD rate, EnDTR and EnDn are found, but the lowest decrement in the temperature of the hot fluid is recorded with the maximum flow rate of cold fluid i.e. 0.037 kg/s. But these outputs are also not good for a heat exchanger. At this operating condition, the performance of heat exchanger is poor and it should be ignored.

Comparative percentage change in the performance evaluation characteristics during experimental analyses 1–2, 3–4, 5–6, 7–8, 9–10, 11–12 and 13–14 are shown in Figs. 6 and 7 respectively. It has been observed after analyses of various experiments (with same flow rates of hot and cold fluids i.e. experiments 1–2) the highest temperature differences in the hot and cold fluids generally give maximum rates of entropy generation and exergy destruction but minimum rate of entransy dissipation for the fabricated shell and spiral tube heat exchanger. Maximum percentage change in the effectiveness has been found during experiments 9–10 because there was the maximum temperature difference in hot fluid. Maximum percentage changes in the rate of exergy destruction and decrement/increment in temperatures of hot/cold fluids have been found during experiments 5–6 because

Table 2 Theoretical outputs for the shell and spiral tube heat exchanger

Sr. No	Parameters	Findings
1	Length of the spiral tube	2513.2 mm
2	Pitch of the tube	251.3 mm
3	Tube side Reynolds’s number	46.02×10^4
4	Pressure drop	4084.467 N/m ²
5	Nusselt number	1574.14/42.82
6	Prandlt number	6.06
7	Convective heat transfer coefficient	87.70×10^3 W/m ² K

Table 3 Properties for the shell and spiral tube heat exchanger

Sr. no	Properties for heat exchanger	Values
1	Number of turns of the spiral tube	10
2	Density of the fluid	997.5 kg/m ³
3	Velocity of the fluid through the spiral tube	37.29 m/s
4	Dynamic viscosity	0.0008891 N-s/m ²
5	Friction coefficient	0.00235
6	Number of spiral tube	1
7	Specific heat of flowing fluid	4178 J/kg-K
8	Thermal conductivity of flowing fluid	0.6129 W/m-K
9	Spiral tube and coil diameters	0.011 and 0.088 m

Table 4 Effectiveness of shell and spiral tube heat exchanger at different operating conditions

Sr. no	Flow rate of cold fluid (kg/s)	Flow rate of hot fluid (kg/s)	Inlet temperature of hot fluid (°C)	Inlet temperature of cold fluid (°C)	Outlet temperature of hot fluid (°C)	Outlet temperature of cold fluid (°C)	Effectiveness
Experiment 1	0.036	0.0028	58	24	27	26.5	0.911
Experiment 2	0.036	0.0028	59	26	26.8	28.5	0.975
Experiment 3	0.0184	0.0018	56	26	27.7	28.7	0.943
Experiment 4	0.0184	0.0018	58	26.5	28.4	29.5	0.939
Experiment 5	0.032	0.0066	56	24	29.5	29.3	0.828
Experiment 6	0.032	0.0066	52	24.5	30.5	28.9	0.781
Experiment 7	0.028	0.0012	65	26.5	30	28	0.909
Experiment 8	0.028	0.0012	63	26.4	31.7	27.8	0.855
Experiment 9	0.018	0.0006	60	26.7	29.1	27.7	0.927
Experiment 10	0.018	0.0006	55	25.8	29.9	26.6	0.859
Experiment 11	0.031	0.0009	60	26.6	27.1	27.6	0.985
Experiment 12	0.031	0.0009	64	26.8	27.6	27.9	0.978
Experiment 13	0.037	0.001	59	26.8	27.2	27.7	0.988
Experiment 14	0.037	0.001	58	26.7	27.1	27.5	0.987

maximum temperature differences were recorded in hot and cold fluids.

After analyses of results it has been found that the maximum effectiveness but minimum EnD rate, EnDTR and EnDn for fabricated shell and spiral tube heat exchanger were achieved at maximum flow rate of cold fluid and it was good for a heat exchanger. Minimum effectiveness and temperature decrement in hot fluid were recorded at maximum flow rate of hot fluid. The maximum EG rate has been found at maximum flow rates of fluids which was not a fine condition for heat exchanger. The ExD and EG rates should be as low as possible and these conditions were achieved at the lowest flow rates of fluids. Highest increment in the effectiveness of the heat exchanger has been attained with maximum flow rates of the fluids and maximum increment in the inlet temperature

of hot fluid. Lowest increment in the effectiveness has been recorded with maximum flow rate of the cold fluid and minimum increments in the inlet temperatures of hot and cold fluids. Greatest increment in the ExD rate has been observed with maximum flow rates of fluids and comparatively lower inlet temperatures of fluids. The smallest destruction rate has been achieved at the maximum temperature difference between the inlet temperatures of hot and cold fluids. Similar behavior has been observed with the percentage decrement in the temperature of hot fluid. Maximum increments for EnD rate, EnDTR and EDN have been identified with the maximum temperature difference between the inlet temperatures of hot and cold fluids. So the performance of the heat exchanger was based on the inlet temperatures and flow rates of hot and cold fluids.

Table 5 Entropy, exergy and entransy analyses of shell and spiral tube heat exchanger at different operating conditions

Sr. no	EG rate (W/K)	ExD rate (W)	EnD rate (W-K)	EnDTR (K/W)	EnDn (i.e. EDN)	EGN
Experiment 1	0.110	19.747	2268.236	0.017	0.184	0.009
Experiment 2	0.059	18.338	6095.886	0.043	0.490	0.005
Experiment 3	0.015	9.661	4667.123	0.103	0.731	0.002
Experiment 4	0.062	10.486	969.029	0.020	0.138	0.008
Experiment 5	0.049	36.888	18,400.058	0.034	0.787	0.002
Experiment 6	0.076	27.262	10,003.448	0.028	0.614	0.003
Experiment 7	0.036	10.915	3553.389	0.115	0.526	0.007
Experiment 8	0.055	9.797	1121.484	0.046	0.195	0.011
Experiment 9	0.006	4.173	2021.220	0.337	0.784	0.003
Experiment 10	0.002	3.211	1847.499	0.467	1.006	0.001
Experiment 11	0.040	6.319	292.232	0.019	0.071	0.011
Experiment 12	0.045	7.765	843.760	0.045	0.166	0.012
Experiment 13	0.043	6.545	224.171	0.013	0.052	0.010
Experiment 14	0.003	6.223	3624.561	0.217	0.897	0.001

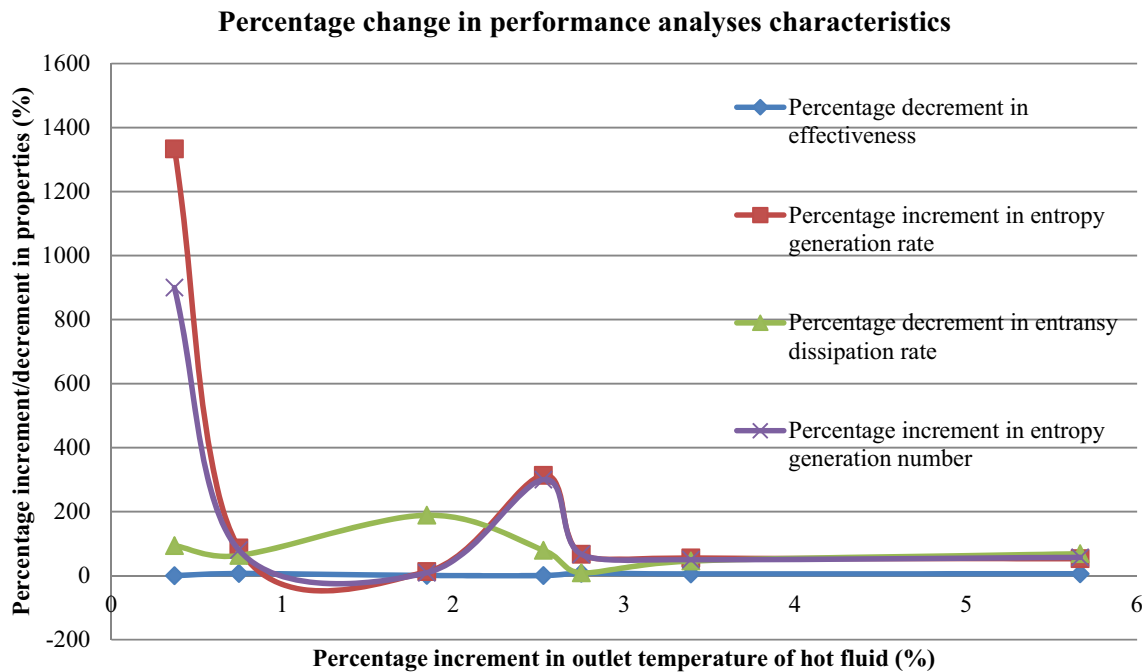


Fig. 5 Percentage change in performance analyses characteristics

Conclusions

Reynolds number, Nusselt number, friction factor, convective heat transfer coefficient and pressure drop through the spiral tube are found theoretically. Then the rates of EG, ExD, EnD, EnDTRs, EnDns, EGNs and effectiveness are evaluated for the fabricated heat exchanger experimentally. It is reviewed that the effectiveness should be as

high as achievable but EG, ExD, EnD, EnDTR, EnDn and EGN should be as low as possible for better performance of heat exchangers. After analyses, this experimental research work can be concluded as; (a) the least EnD rate (i.e. 224.171 W-K), EnDTR (i.e. 0.013 K/W) and EnDn (i.e. 0.052) are found during experiment number 13 that shows maximum and minimum flow rates of cold and hot fluids with the highest effectiveness which is excellent for a heat

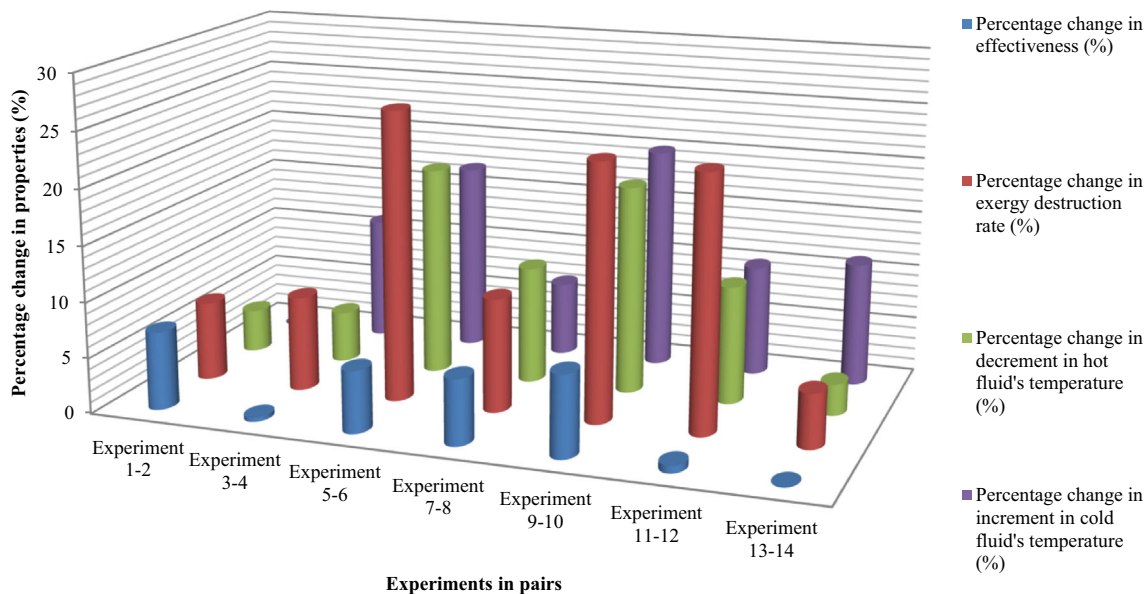


Fig. 6 Percentage change in effectiveness, ExD and fluid temperatures at different experimental pairs

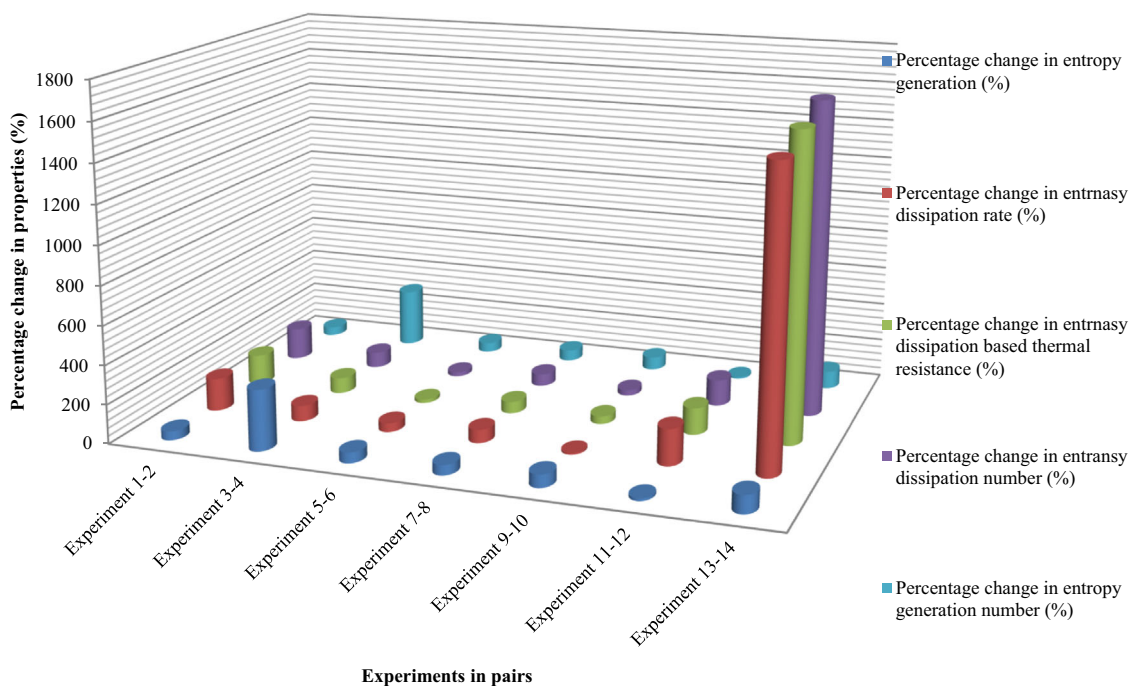


Fig. 7 Percentage change in EG, EnD, thermal resistance, EnD and EGNs at different experimental pairs

exchanger. (b) Least effectiveness (i.e. 0.781) of the heat exchanger is found in experiment number 6 with the lowest inlet temperatures of the hot and cold fluids. (c) Entropy generation rate (i.e. 0.076 W/K), exergy destruction rate (i.e. 27.262 W) and entransy dissipation rate (i.e. 10,003.448 W-K) are also maximum in experiment 6 and these outputs are not good for a heat exchanger. (d) The

greater rates of ExD (i.e. 36.888 W) and EnD (i.e. 18,400.058 W-K) are not favorable situations for better outputs. (e) Highest increments in the EnD rate (i.e. 1516.87%), EnDTR (i.e. 1569.23%) and EnDn (i.e. 1625%) are found, but the lowest decrement in the temperature of the hot fluid is recorded with the maximum flow rate of cold fluid i.e. 0.037 kg/s. (f) Maximum increments

in the effectiveness (i.e. 7.364%) and the temperature of cold fluid (i.e. 20%) are achieved, but minimum increment in EnD rate (i.e. 8.594%) is observed with the smallest flow rates of cold and hot fluids i.e. 0.018 and 0.0006 kg/s respectively. (g) When the flow rates of cold and hot fluids are raised slightly upto 0.0184 and 0.0018 kg/s then maximum increments in EG rate (i.e. 313.33%) and EGN (i.e. 300%) are found which were also not admirable. After comparative experimental analyses, operating conditions of experiments 11–14 are recommended for the fabricated shell and spiral tube heat exchanger which give maximum possible values of effectiveness for the heat exchanger but the minimum rate of EnD, EnDTR, EnDn and EGN. Copper should be used as spiral tube material because it has maximum thermal conductivity which is the basic requirement for heat transfer process between two flowing fluids. For better performance of the heat exchangers, one fluid should be flow with maximum rate and other fluid should flow with minimum rate. Both fluids should not flow with extreme flow rates, however minimum flow rates of fluids are recommended for better performance from any heat exchanger.

Acknowledgment This work was done at Sushila Devi Bansal College of Technology, Indore, India. There is no conflict of interest. This research did not receive any specific grant from funding agencies.

Declarations

Conflict of interest The authors declare that they have no conflict of interest.

References

1. J.P. Holman, S. Bhattacharyya, *Heat Transfer*, 10th edn. (Tata McGraw Hill Education, New Delhi, India, 2011).
2. Y.A. Cengel, *Heat Transfer: A Practical Approach*, 2nd edn. (Tata McGraw Hill Publication, New Delhi, India, 2002).
3. H.J. Lienhard, *A Heat Transfer Text Book* (Phlogiston Press, Cambridge, 2008).
4. R.K. Shah, D.P. Sekulic, *Fundamental of Heat Exchanger Design*, 10th edn. (Wiley, Hoboken, NJ, 2003).
5. S. Whitaker, *Fundamental Principles of Heat Transfer* (Florida: Robert E Krieger Publishing Company, Inc., Krieger Drivemalabar, 1983).
6. G.F. Hewitt, G.L. Shires, T.B. Bott, *Process Heat Transfer*, 1st edn. (Taylor & Francis Group USA CRC Pres, Boca Raton, 1994).
7. L.G. Chen, K. Ma, Y.L. Ge, F.R. Sun, Minimum entropy generation path for an irreversible light-driven engine with reacting system and linear phenomenological heat transfer law. *Environ. Eng. Manag. J.* **16**(9), 2035–2043 (2017)
8. L.G. Chen, S.J. Xia, F.R. Sun, Entropy generation minimization for isothermal crystallization processes with a generalized mass diffusion law. *Int. J. Heat Mass Transf.* **116**, 1–8 (2018)
9. L.G. Chen, L. Zhang, S.J. Xia, F.R. Sun, Entropy generation minimization for hydrogenation of CO₂ to light olefins. *Energy* **147**, 187–196 (2018)
10. A. Bejan, *Entropy Generation Through Heat and Fluid Flow* (Wiley, New York, 1982).
11. A. Geete, Exergy, entransy and entransy based thermal resistance analyses of double pipe heat exchanger with different pipe materials. *Heat Transf. Res.* **48**(18), 1625–1636 (2017). <https://doi.org/10.1615/HeatTransRes.2017015641>
12. I.L. Paniagua, J.R. Martin, C.G. Fernandez, A.J. Alvaro, R.N. Carlier, A new simple method for estimating ExD in heat exchangers. *Entropy* **15**, 474–489 (2013)
13. L.G. Chen, Q.H. Xiao, H.J. Feng, Constructural optimizations for heat and mass transfers based on the EnD extremum principle, performed at the Naval Univerisity of Engineering: a review. *Entropy* **20**(1), 74 (2018)
14. X.T. Cheng, X.G. Liang, Entransy, entransy dissipation and entransy loss for analyses of heat transfer and heat-work conversion processes. *J. Therm. Sci. Technol.* **8**(2), 337–352 (2013)
15. H.J. Feng, L.G. Chen, Z.H. Xie, Constructural optimizations for “+” shaped high conductivity channels based on EnD rate minimization. *Int. J. Heat Mass Transf.* **119**, 640–646 (2018)
16. Z.Y. Guo, H.Y. Zhu, X.G. Liang, Entransy—A physical quantity describing heat transfer ability. *Int. J. Heat Mass Transf.* **50**, 2545–2556 (2007)
17. C. Wang, Y. Zhu, Entransy analysis on boiler air pre-heater with multi-stage LHS unit. *Appl. Therm. Eng.* **130**, 1139–1146 (2018)
18. J.F. Guo, L. Cheng, M.T. Xu, Entransy dissipation number and its application to heat exchanger performance evaluation. *Chin. Sci. Bull.* **54**(15), 2708–2713 (2009)
19. K.H. Kim, S.W. Kim, EnD analysis for optimal design of heat exchangers. *J. Autom. Control Eng.* **03**(02), 87–91 (2015)
20. X. Liu, F. Wang, Z. Li, C. Zhu, H. Zhang, H. Zhang, Parametric investigation of thermal-hydrodynamic performance in the innovative helical coiled heat exchangers in the heat pump system. *Energy Build.* **216**(1), 109961 (2020)
21. A.S. Bakir, H.B. Mahood, A.R. Kareem, Optimization and evaluation of NTU and effectiveness of a helical coil tube heat exchanger with air injection. *Therm. Sci. Eng. Process.* **14**, 100420 (2019)
22. N.H. Abu-Hamdeh, R.A.R. Bantan, I. Tlili, Analysis of the thermal and hydraulic performance of the sector-by-sector helical coil tube heat exchangers as a new type of heat exchangers. *Int. J. Therm. Sci.* **150**, 106229 (2020)
23. P.C.M. Kumar, M. Chandrasekar, A review on helically coiled tube heat exchanger using nanofluids. *Mater. Today Proc.* **21**(1), 137–141 (2020)
24. G. Wang, T. Dbouk, D. Wang, Y. Pei, X. Peng, H. Yuan, S. Xiang, Experimental and numerical investigation on hydraulic and thermal performance in the tube-side of helically coiled-twisted trilobal tube heat exchanger. *Int. J. Therm. Sci.* **153**, 106328 (2020)
25. P.C.M. Kumar, M. Chandrasekar, CFD analysis on heat and flow characteristics of double helically coiled tube heat exchanger handling MWCNT/water nanofluids. *Heliyon* **5**(7), e02030 (2019)
26. H. Mirgolbabaee, Numerical investigation of vertical helically coiled tube heat exchangers thermal performance. *Appl. Therm. Eng.* **136**, 252–259 (2018)
27. G. Wang, D. Wang, J. Deng, Y. Lyu, Y. Pei, S. Xiang, Experimental and numerical study on the heat transfer and flow characteristics in shell side of helically coiled tube heat exchanger based on multi-objective optimization. *Int. J. Heat Mass Transf.* **137**, 349–364 (2019)
28. A.K. Solanki, R. Kumar, Condensation frictional pressure drop characteristic of R-600a inside the horizontal smooth and dimpled helical coiled tube in shell type heat exchanger. *Int. J. Therm. Sci.* **154**, 106406 (2020)

29. Y. Han, X. Wang, H. Zhang, Q. Chen, Z. Zhang, Multi-objective optimization of helically coiled tube heat exchanger based on entropy generation theory. *Int. J. Therm. Sci.* **147**, 106150 (2020)
30. E. Gholamalizadeh, E. Hosseini, M.B. Jamnani, A. Amiri, A.D. Saeed, A. Alimoradi, Study of intensification of the heat transfer in helically coiled tube heat exchangers via coiled wire inserts. *Int. J. Therm. Sci.* **141**, 72–83 (2019)
31. V. Saydam, M. Parsazadeh, M. Radeef, X. Duan, Design and experimental analysis of a helical coil phase change heat exchanger for thermal energy storage. *J. Energy Storage* **21**, 9–17 (2019)
32. G. Wang, D. Wang, X. Peng, L. Han, S. Xiang, F. Ma, Experimental and numerical study on heat transfer and flow characteristics in the shell side of helically coiled trilobal tube heat exchanger. *Appl. Therm. Eng.* **149**, 772–787 (2019)
33. A. Sheeba, C.M. Abhijith, M.J. Prakash, Experimental and numerical investigations on the heat transfer and flow characteristics of a helical coil heat exchanger. *Int. J. Refrig.* **99**, 490–497 (2019)
34. M. Omid, M. Farhadi, A.A.R. Darzi, Numerical study of heat transfer on using lobed cross sections in helical coil heat exchangers: effect of physical and geometric parameters. *Energy Convers. Manag.* **176**, 236–245 (2018)
35. T. Mohapatra, B.N. Padhi, S.S. Sahoo, Analytical investigation and performance optimization of a three fluid heat exchanger with helical coil insertion for simultaneous space heating and water heating. *Heat Mass Transf.* **55**, 1723–1740 (2019)
36. R. Kareem, Optimization of double pipe helical tube heat exchanger and its comparison with straight double tube heat exchanger. *J. Inst. Eng. India Ser. C* **98**, 587–593 (2017)
37. R. Kong, A. Asanakhani, T. Kiatsiriroat, Heat transfer characteristics of deionized water-based graphene nanofluids in helical coiled heat exchanger for waste heat recovery of combustion stack gas. *Heat Mass Transf.* **55**, 385–396 (2019)
38. A. Verma, M. Kumar, A.K. Patil, Enhanced heat transfer and frictional losses in heat exchanger tube with modified helical coiled inserts. *Heat Mass Transf.* **54**, 3137–3150 (2018)
39. A.E. Moghadam, F. Gohari, M.D. Dashtebayaz, A comprehensive thermo-hydraulic analysis and optimization of turbulent TiO₂/W-EG nano-fluid flow inside double pipe heat exchangers with helical coil inserts. *J. Braz. Soc. Mech. Sci. Eng.* **42**, 232 (2020)
40. H.F. Elattar, A. Fouda, S.A. Nada, H.A. Refaey, A. Al-Zahrani, Thermal and hydraulic numerical study for a novel multi tubes in tube helically coiled heat exchangers: effects of operating/geometric parameters. *Int. J. Therm. Sci.* **128**, 70–83 (2018). <https://doi.org/10.1016/j.ijthermalsci.2018.02.020>
41. N. Ghorbani, H. Taherian, M. Gorji, H. Mirgolbabaee, An experimental study of thermal performance of shell-and-coil heat exchangers. *Int. Commun. Heat Mass Transf.* **37**(7), 775–781 (2010). <https://doi.org/10.1016/j.icheatmasstransfer.2010.02.001>
42. A. Fouda, S.A. Nada, H.F. Elattar, H.A. Refaey, A.S. Bin-Mahfouz, Thermal performance modeling of turbulent flow in multi tube in tube helically coiled heat exchangers. *Int. J. Mech. Sci.* **135**, 621–638 (2018). <https://doi.org/10.1016/j.jmeasci.2017.12.015>
43. D.Q. Kern, *Process Heat Transfer*, 1st edn. (Tata McGraw Education, New Delhi, 2004).
44. Y.A. Cengel, M.A. Boles, *Thermodynamic: An Engineering Approach*, 7th edn. (Tata McGraw Hill, New Delhi, 2011).
45. A. Geete, Application of exergy and entransy concepts to analyses performance of coal fired thermal power plant: a case study. *Int. J. Ambient Energy* (2019). <https://doi.org/10.1080/01430750.2019.1586762>
46. D. Domkundwar, *Heat and Mass Transfer: Data Book* (Springer, Delhi, 2014).
47. D. Malakar, A. Geete, Application of entropy and entransy concepts to design shell-spiral tube type surface condenser at different 4L/D ratios for Maral Overseas Ltd. *Int. J. Ambient Energy* (2018). <https://doi.org/10.1080/01430750.2018.1490353>
48. A. Geete, V. Patel, S.S. Tanwar, S. Kushwah, N.S. Lodhi, V. Kushwah, Thermodynamic analysis of designed and fabricated shell-spiral tube type heat exchanger by DSTHE software: KERN method. *Int. J. Ambient Energy* **39**(4), 343–351 (2018). <https://doi.org/10.1080/01430750.2017.1303637>
49. A. Geete, R. Pathak, Effect of surface roughness on the performance of heat exchanger. *SN Appl. Sci.* (2019). <https://doi.org/10.1007/s42452-019-0954-x>
50. A. Geete, Comparative performance analysis of concentric tube type heat exchanger at various operating conditions with copper and aluminum tube materials. *Int. J. Ambient Energy* **39**(5), 446–455 (2018). <https://doi.org/10.1080/01430750.2017.1318783>
51. A. Geete, A. Mahajan, A. Shinde, D. Modak, Experimental exergy and entransy analyses on designed and fabricated cross-flow heat exchanger. *Heat Transfer* (2020). <https://doi.org/10.1002/htj.21952>
52. A. Geete, D. Kharve, H. Patel, H. Karma, A. Prajapati, S. Sharma, Comparative exergy and exergy efficiency analyses of fabricated single and double slope solar still plants at Indore: case study. *SN Appl. Sci.* **2**, 963 (2020). <https://doi.org/10.1007/s42452-020-2763-7>

Publisher's Note Springer Nature remains neutral with regard to jurisdictional claims in published maps and institutional affiliations.